Figure S.1

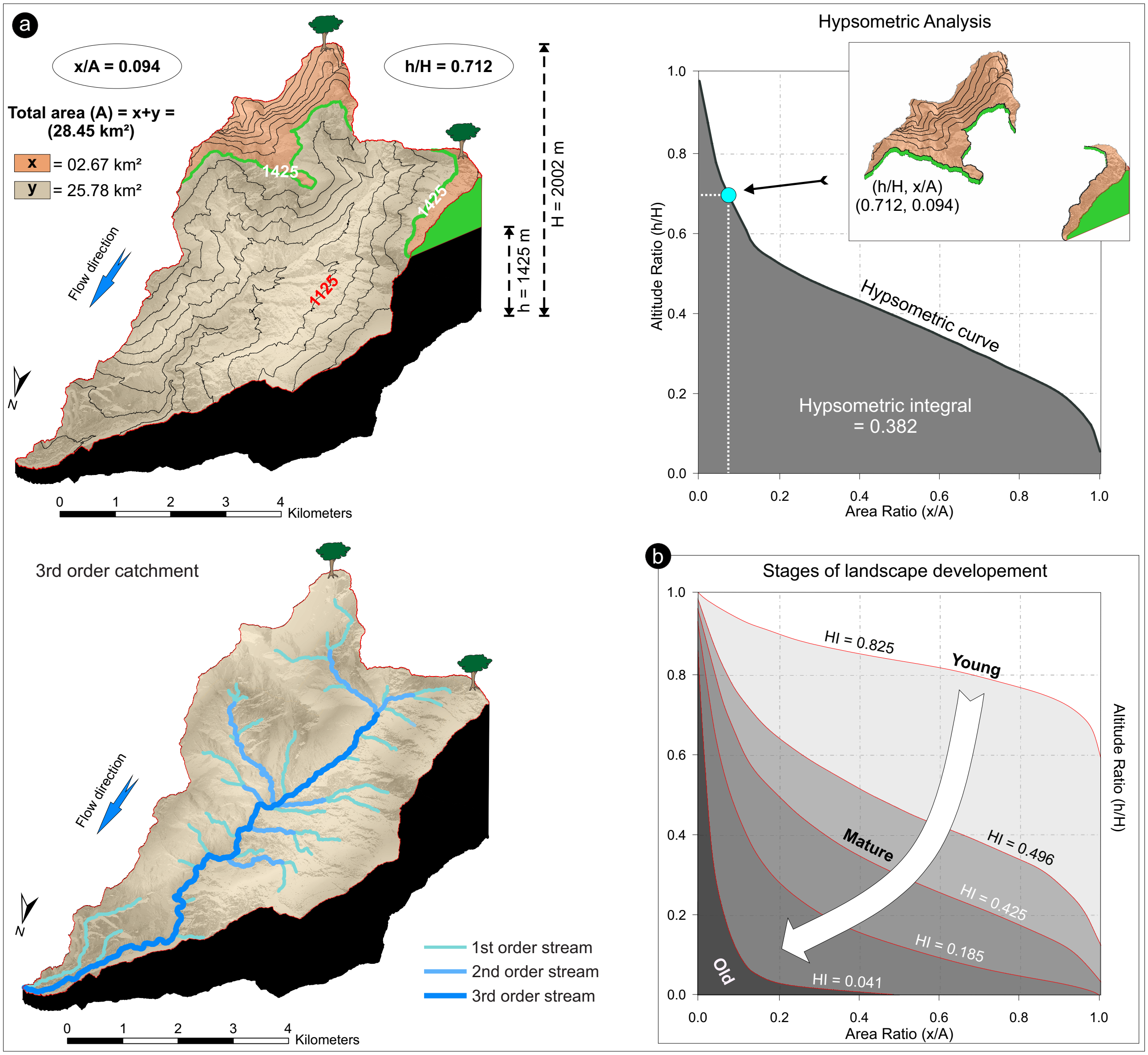
a
x/A = 0.094
h/H = 0.712
Total area (A) = x+y = (28.45 km²)
x = 02.67 km²
y = 25.78 km²
1425
1425
1125
h = 1425 m
H = 2002 m
Flow direction
N
0 1 2 3 4 Kilometers
Hypsometric Analysis
(h/H, x/A)
(0.712, 0.094)
Hypsometric curve
Hypsometric integral
= 0.382
Altitude Ratio (h/H)
Area Ratio (x/A)
3rd order catchment
Flow direction
1st order stream
2nd order stream
3rd order stream
b
Stages of landscape developement
HI = 0.825
Young
Mature
HI = 0.496
HI = 0.425
HI = 0.185
HI = 0.041
Old
Altitude Ratio (h/H)
Area Ratio (x/A)

Fig. S.1. (a) Schematic diagram illustrating the way to construct a hypsometric curve for 3rd order drainage catchment (no. 45, Fig. 7) based on the method described by Strahler (1952). The area under the curve, described by the hypsometric integral (0.382), reflecting the amount of materials hasn't yet been eroded or transformed. (b) Hypsometric curves, illustrating a landscape aging cycle (adapted from Strahler, 1952).

Figure S.2

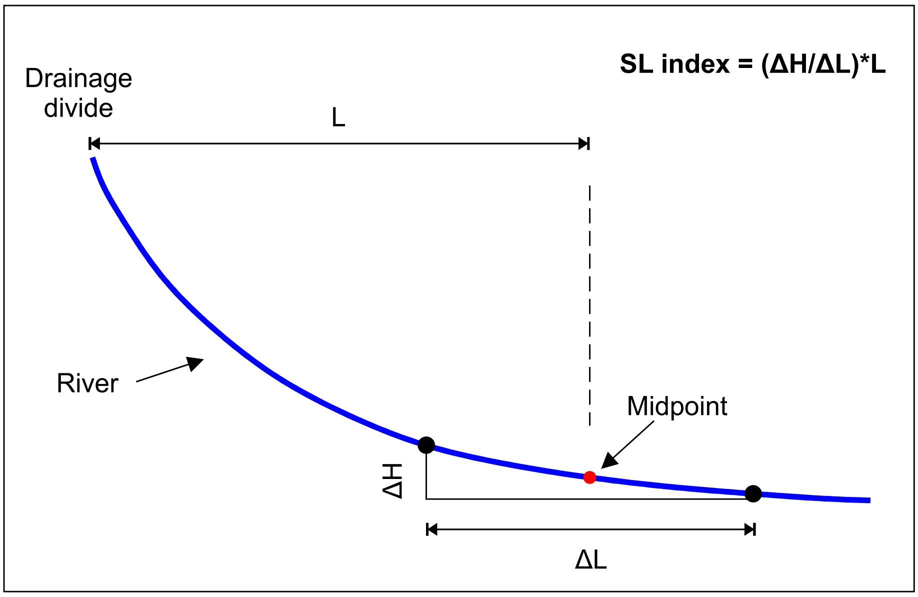

Fig. S.2. A scheme showing the parameters used in the calculation of SL index (after Hack, 1973). ΔH is the difference in elevation between the ends of the segment, ΔL is the length of the segment, and L is the total length from the drainage divide to the midpoint of the segment.

Figure S.3

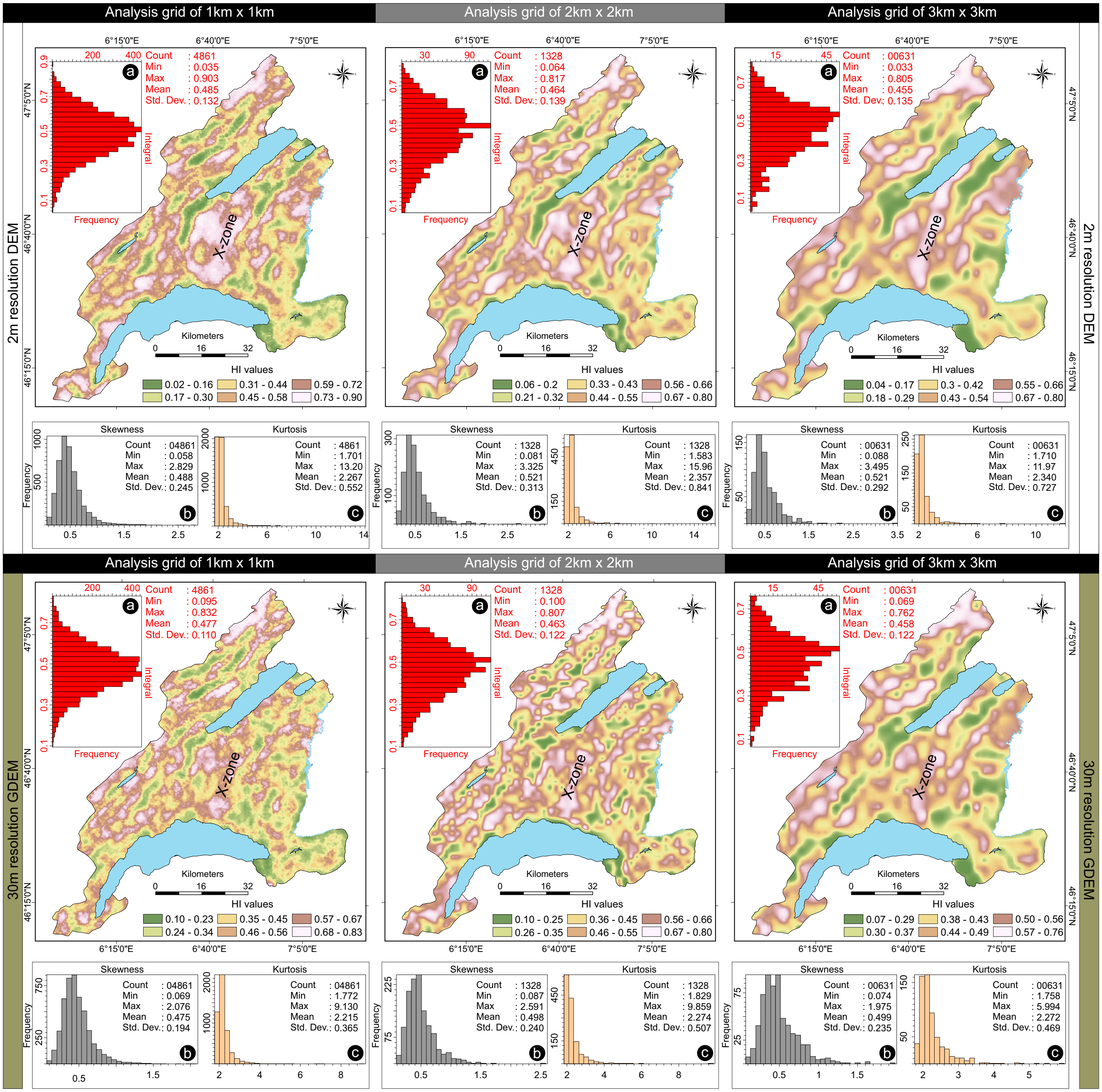

Analysis grid of 1km x 1km
Analysis grid of 2km x 2km
Analysis grid of 3km x 3km
2m resolution DEM
30m resolution GDEM
6°15'0"E
6°40'0"E
7°5'0"E
47°5'0"N
46°40'0"N
46°15'0"N
Count : 4861
Min : 0.035
Max : 0.903
Mean : 0.485
Std. Dev.: 0.132
Count : 1328
Min : 0.064
Max : 0.817
Mean : 0.464
Std. Dev.: 0.139
Count : 00631
Min : 0.033
Max : 0.805
Mean : 0.455
Std. Dev.: 0.135
Frequency
Integral
X-zone
Kilometers
0 16 32
HI values
0.02 - 0.16
0.17 - 0.30
0.31 - 0.44
0.45 - 0.58
0.59 - 0.72
0.73 - 0.90
0.06 - 0.2
0.21 - 0.32
0.33 - 0.43
0.44 - 0.55
0.56 - 0.66
0.67 - 0.80
0.04 - 0.17
0.18 - 0.29
0.3 - 0.42
0.43 - 0.54
0.55 - 0.66
0.67 - 0.80
Skewness
Kurtosis
Count : 04861
Min : 0.058
Max : 2.829
Mean : 0.488
Std. Dev.: 0.245
Count : 4861
Min : 1.701
Max : 13.20
Mean : 2.267
Std. Dev.: 0.552
Count : 1328
Min : 0.081
Max : 3.325
Mean : 0.521
Std. Dev.: 0.313
Count : 1328
Min : 1.583
Max : 15.96
Mean : 2.357
Std. Dev.: 0.841
Count : 00631
Min : 0.088
Max : 3.495
Mean : 0.521
Std. Dev.: 0.292
Count : 00631
Min : 1.710
Max : 11.97
Mean : 2.340
Std. Dev.: 0.727
Count : 4861
Min : 0.095
Max : 0.832
Mean : 0.477
Std. Dev.: 0.110
Count : 1328
Min : 0.100
Max : 0.807
Mean : 0.463
Std. Dev.: 0.122
Count : 00631
Min : 0.069
Max : 0.762
Mean : 0.458
Std. Dev.: 0.122
0.10 - 0.23
0.24 - 0.34
0.35 - 0.45
0.46 - 0.56
0.57 - 0.67
0.68 - 0.83
0.10 - 0.25
0.26 - 0.35
0.36 - 0.45
0.46 - 0.55
0.56 - 0.66
0.67 - 0.80
0.07 - 0.29
0.30 - 0.37
0.38 - 0.43
0.44 - 0.49
0.50 - 0.56
0.57 - 0.76
Count : 04861
Min : 0.069
Max : 2.076
Mean : 0.475
Std. Dev.: 0.194
Count : 04861
Min : 1.772
Max : 9.130
Mean : 2.215
Std. Dev.: 0.365
Count : 1328
Min : 0.087
Max : 2.591
Mean : 0.498
Std. Dev.: 0.240
Count : 1328
Min : 1.829
Max : 9.859
Mean : 2.274
Std. Dev.: 0.507
Count : 00631
Min : 0.074
Max : 1.975
Mean : 0.499
Std. Dev.: 0.235
Count : 00631
Min : 1.758
Max : 5.994
Mean : 2.272
Std. Dev.: 0.469

Fig. S.3. Spatial distribution of the hypsometric integral with the main statistics of the hypsometric attributes (frequency-histograms) obtained by using two different resolution DEMs (2 m and 30 m) with three different regularly spaced grids (1 km, 2 km, and 3 km). In all six cases, the statistical distribution of the hypsometric integral values (a) follows the same pattern with a mean average very close to 0.5. The same observation can be highlighted for the hypsometric skewness (b) and hypsometric kurtosis (c) values with a mean average very close to 0.5 and 2.3, respectively. The smallest hypsometric integral values are generally obtained using the 2 m DEM. This is probably because the 2 m DEM provides more detailed information about the existing topographic features than 30 m GDEM. Other significant similarities can also found between the spatial distributions of hypsometric integral values (background images) that obtained when the same/different DEMs and grid size were used. As can be also seen by comparing Figs 5b and S.3, there are several kilometric-scale zones show similar patterns in the distribution of hypsometric integral values. For example, a distinctive zone of higher hypsometric integral values can be observed in the central part of the study area in all seven cases (X-zone in Fig. S.3 and catchments no. 12, 13, 19, 24, 25, 34, 66, 70, 71, 72, and 73 in Fig. 5b). Thus, it can be argued that there is no scale dependence of the hypsometric integral values. These findings, however, correlate well with the results of hypsometric analysis obtained using two different resolution DEMs (10 m and 90 m) with different grid sizes (500 m, 1 km, and 2 km) for the Granada basin in the SE of Spain (Pérez-Peña et al., 2009).

Figure S.4

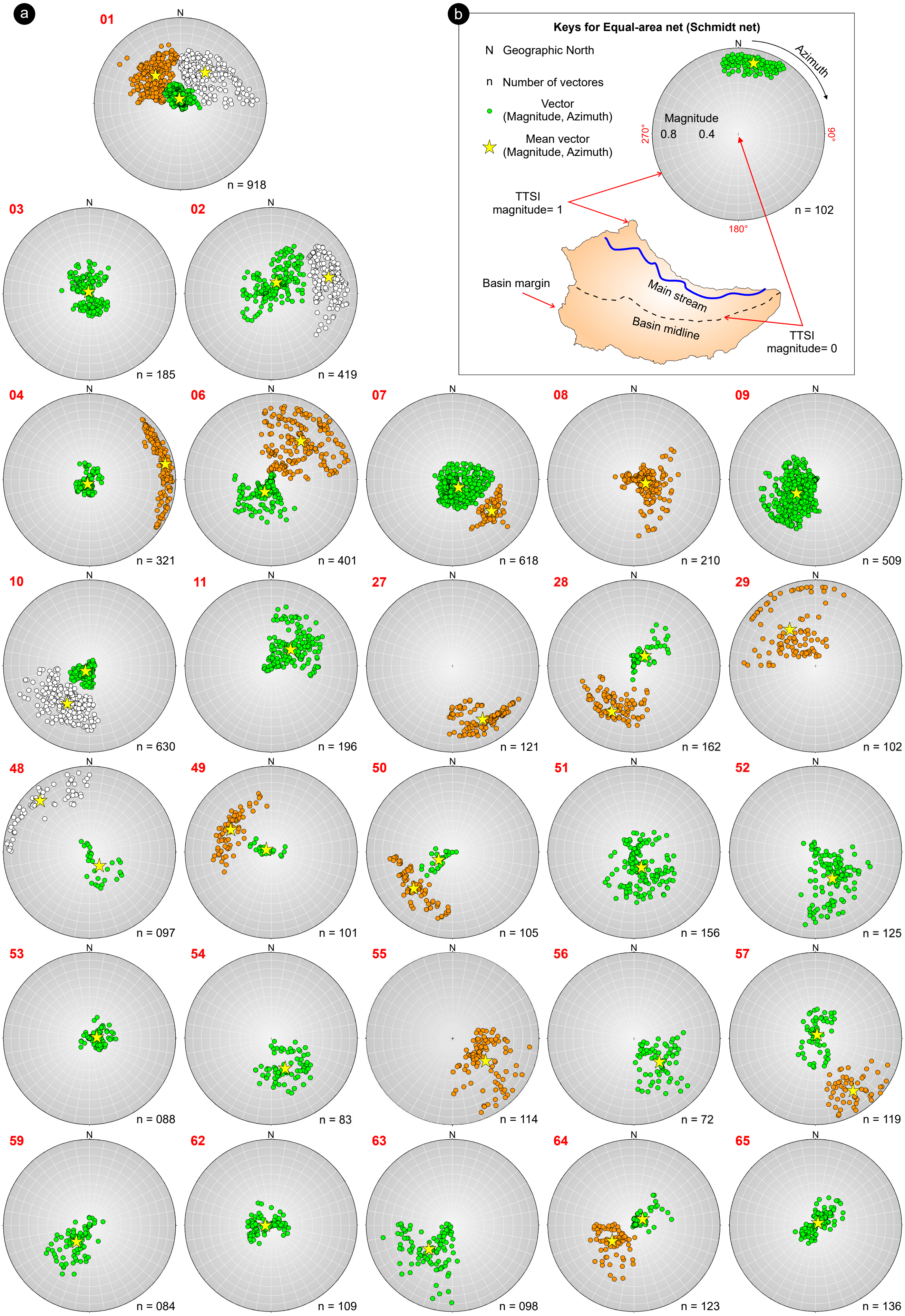

a
01
n = 918
03
n = 185
02
n = 419
04
n = 321
06
n = 401
07
n = 618
08
n = 210
09
n = 509
10
n = 630
11
n = 196
27
n = 121
28
n = 162
29
n = 102
48
n = 097
49
n = 101
50
n = 105
51
n = 156
52
n = 125
53
n = 088
54
n = 83
55
n = 114
56
n = 72
57
n = 119
59
n = 084
62
n = 109
63
n = 098
64
n = 123
65
n = 136
b
Keys for Equal-area net (Schmidt net)
N Geographic North
n Number of vectores
Vector (Magnitude, Azimuth)
Mean vector (Magnitude, Azimuth)
Azimuth
Magnitude
0.8 0.4
270°
90°
180°
n = 102
TTSI magnitude= 1
Basin margin
Main stream
Basin midline
TTSI magnitude= 0

Fig. S.4. (a) Lower-hemisphere, equal-area plots (Schmidt's projection) showing vector values (azimuth/magnitude) of Transverse Topographic Symmetry Index (TTSI) analysis for twenty-eight drainage catchments in the westernmost part of Switzerland (Domain-I). Vectors that agree in terms of the magnitudes and azimuths tend to clusters together in specific groups. The groups with relatively high magnitude values of TTSI indicate a possible number of deflections for the stream. Red number on the upper-left corner of the polar plot indicates the name of catchment. (b) Keys to read stereonet (Schmidt's projection, lower hemisphere). Azimuth values of TTSI (0° to 360°) are indicated along the outermost great circle of the plot, whereas TTSI magnitude (0 to 1) is indicated along the x and y axes. The TTSI magnitude is close/equal to 0 if the river incises along the basin midline, and close/equal to 1 if the river flows near to the basin boundary.

Figure S.5

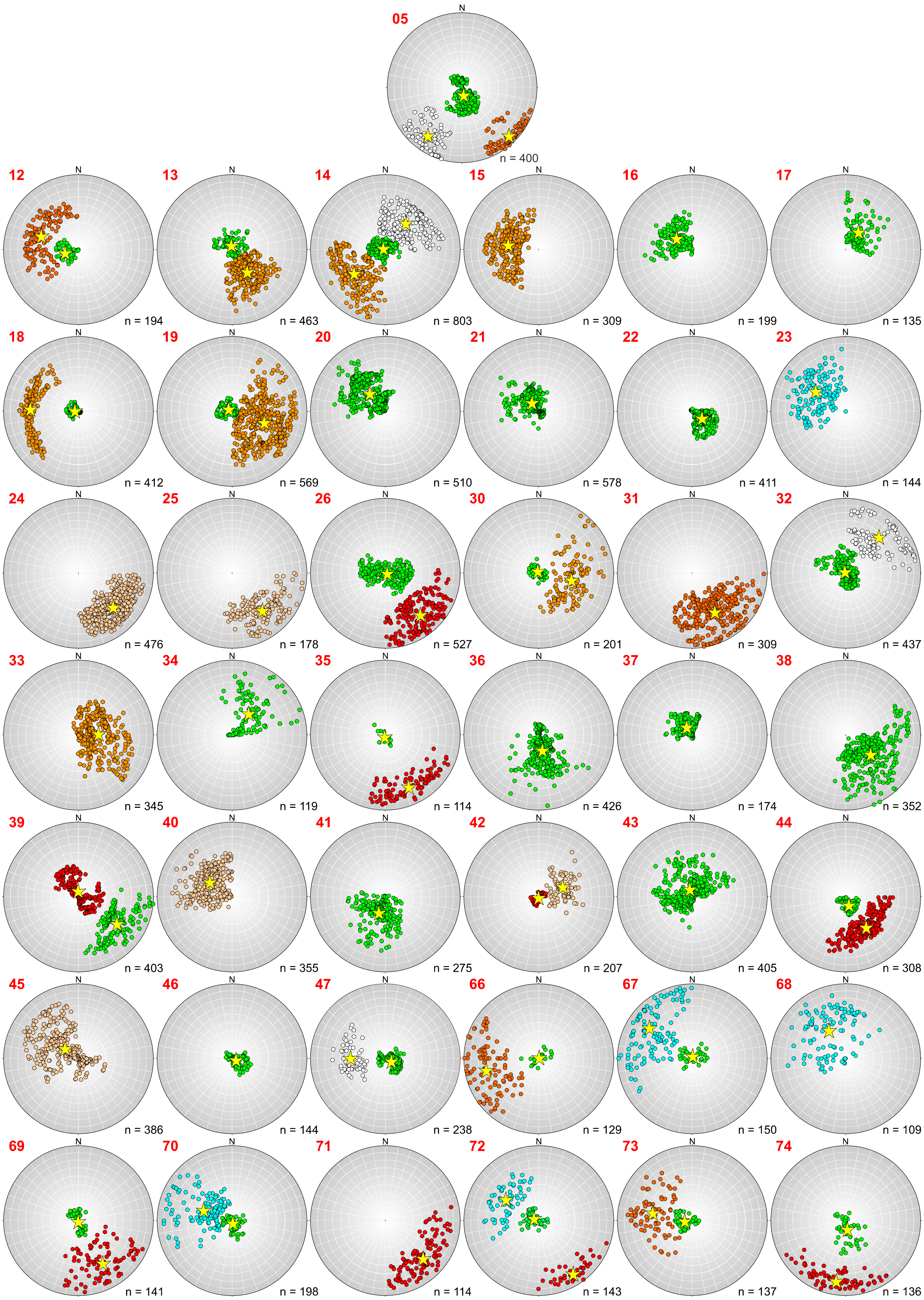

05
N
n = 400
12
n = 194
13
n = 463
14
n = 803
15
n = 309
16
n = 199
17
n = 135
18
n = 412
19
n = 569
20
n = 510
21
n = 578
22
n = 411
23
n = 144
24
n = 476
25
n = 178
26
n = 527
30
n = 201
31
n = 309
32
n = 437
33
n = 345
34
n = 119
35
n = 114
36
n = 426
37
n = 174
38
n = 352
39
n = 403
40
n = 355
41
n = 275
42
n = 207
43
n = 405
44
n = 308
45
n = 386
46
n = 144
47
n = 238
66
n = 129
67
n = 150
68
n = 109
69
n = 141
70
n = 198
71
n = 114
72
n = 143
73
n = 137
74
n = 136

Fig. S.5. Lower-hemisphere, equal-area plots showing vector values (azimuth/magnitude) of Transverse Topographic Symmetry Index (TTSI) analysis for forty-three drainage catchments in the westernmost part of Switzerland (Domain-II). Red number on the upper-left corner of the polar plot indicates the name of catchment. Keys for stereoplot are shown in Fig. S.4b.

Figure S.6

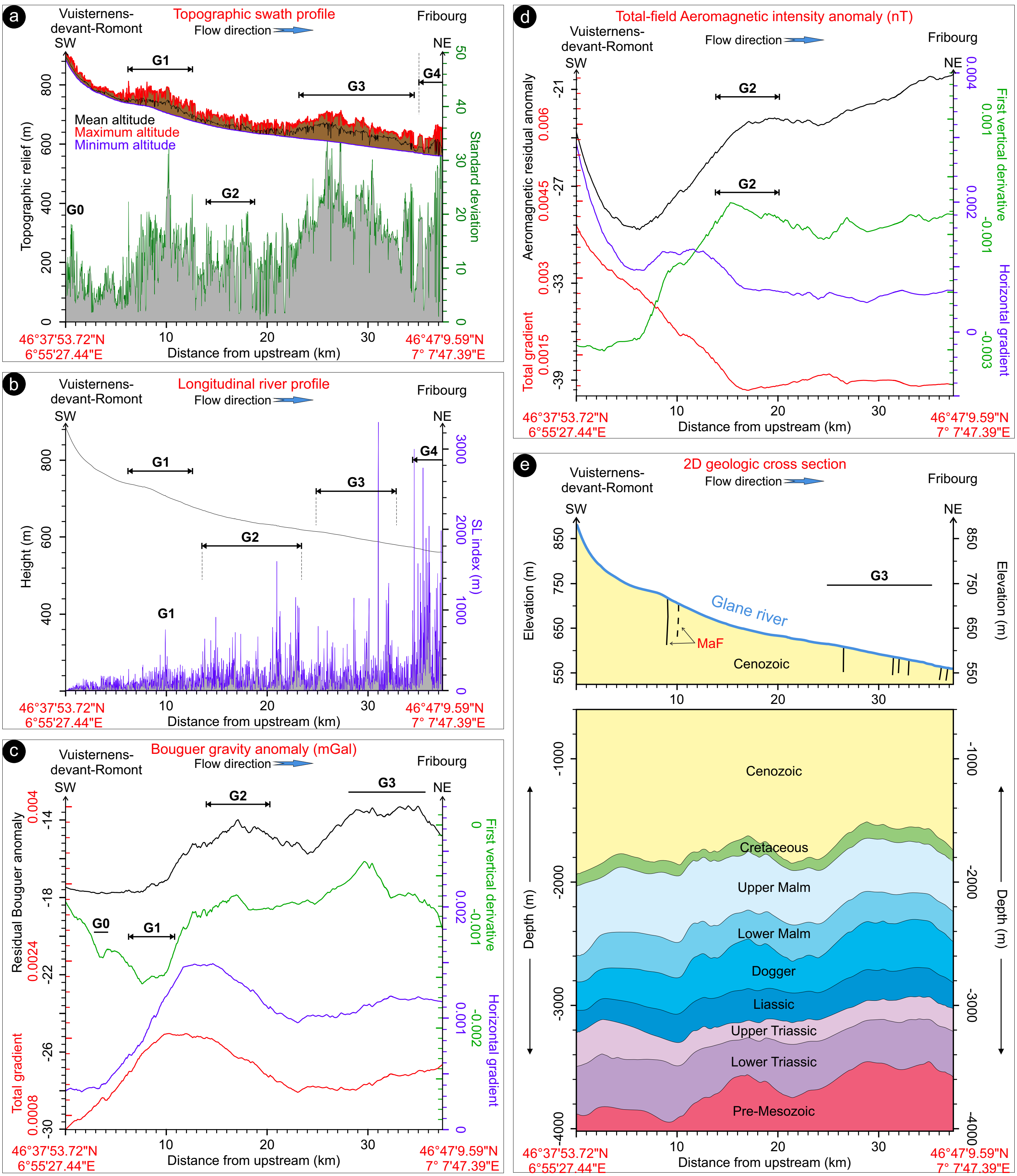

a
Vuisternens-devant-Romont
Topographic swath profile
Flow direction
Fribourg
SW
NE
G0
G1
G2
G3
G4
Mean altitude
Maximum altitude
Minimum altitude
Topographic relief (m)
Standard deviation
46°37'53.72"N 6°55'27.44"E
46°47'9.59"N 7° 7'47.39"E
Distance from upstream (km)
b
Longitudinal river profile
Height (m)
SL index (m)
c
Bouguer gravity anomaly (mGal)
Residual Bouguer anomaly
First vertical derivative
Horizontal gradient
Total gradient
d
Total-field Aeromagnetic intensity anomaly (nT)
Aeromagnetic residual anomaly
e
2D geologic cross section
Glane river
MaF
Elevation (m)
Depth (m)
Cenozoic
Cretaceous
Upper Malm
Lower Malm
Dogger
Liassic
Upper Triassic
Lower Triassic
Pre-Mesozoic

Fig. S.6. Topographical, geophysical, and longitudinal profiles of the entire 37-km length of the Glane river in the westernmost of Switzerland. (a) One-km wide topographic swath profile displaying more than three distinct reliefs along both sides of the river (labeled by G1 – G4). The highest rates of fluvial incision occur in the G1, G3 and G4 zones. Mean elevation curve nearly shows the same pattern of change as maximum altitude curve. (b) Longitudinal profile based on the channel's bottom elevation and gradient (SL index). (c) and (d) Unfiltered and filtered residual gravity and aeromagnetic anomaly profiles along the river path, respectively. (e) Geological cross-section along the river, extracted from a 3D geological model based on the interpretation of seismic reflection data (Gruber, 2017), showing that Mesozoic sequences occur at great depth beneath a thick Cenozoic rocks. Black dashed/solid lines represent proposed/certain faults (Ibele, 2011; Weidmann et al., 2002). MaF: La Mausson strike-slip Fault.

Figure S.7

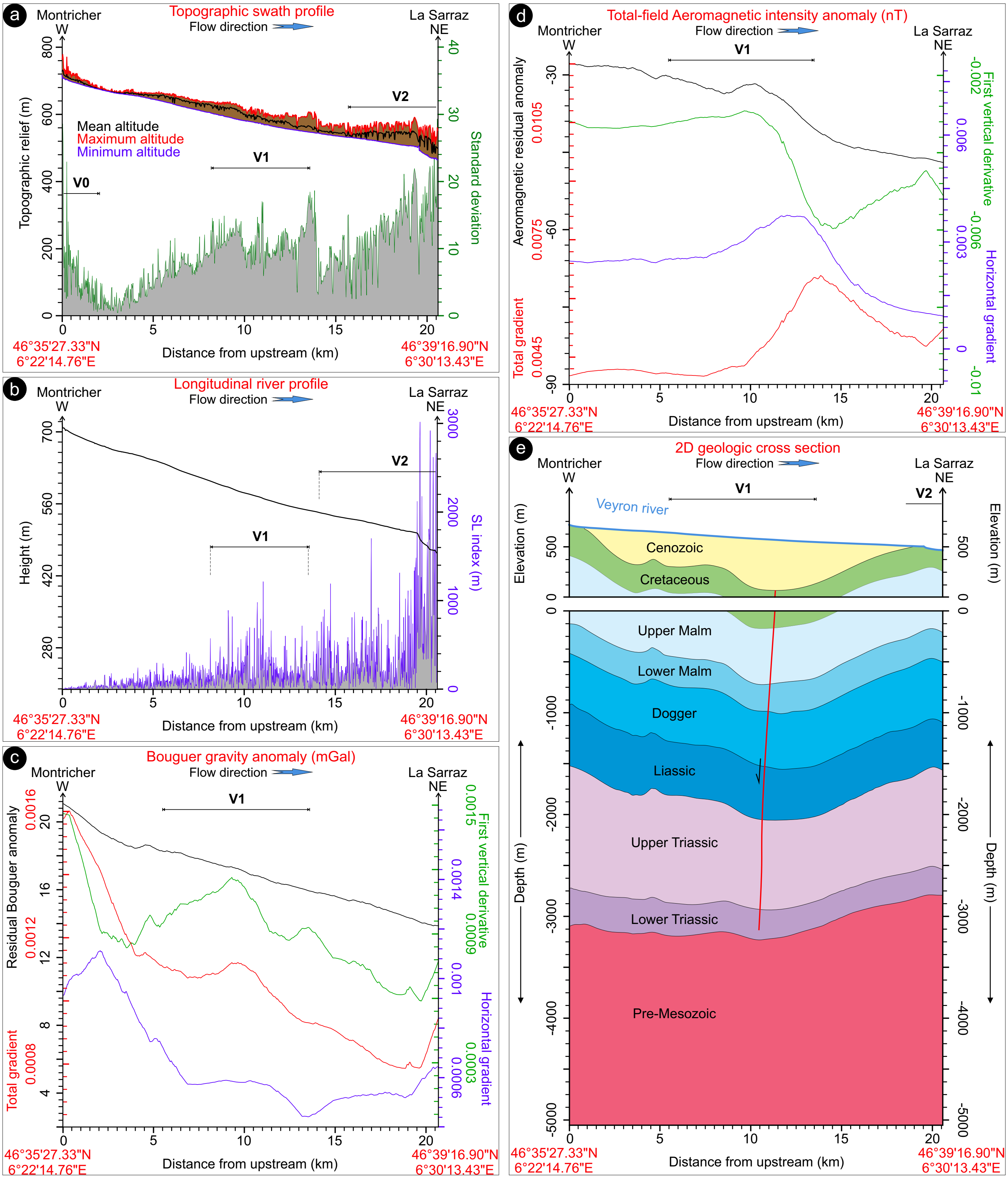

a
Topographic swath profile
Montricher
W
Flow direction
La Sarraz
NE
Mean altitude
Maximum altitude
Minimum altitude
V0
V1
V2
Topographic relief (m)
Standard deviation
Distance from upstream (km)
46°35'27.33"N
6°22'14.76"E
46°39'16.90"N
6°30'13.43"E
b
Longitudinal river profile
Height (m)
SL index (m)
c
Bouguer gravity anomaly (mGal)
Residual Bouguer anomaly
Total gradient
First vertical derivative
Horizontal gradient
d
Total-field Aeromagnetic intensity anomaly (nT)
Aeromagnetic residual anomaly
e
2D geologic cross section
Veyron river
Cenozoic
Cretaceous
Upper Malm
Lower Malm
Dogger
Liassic
Upper Triassic
Lower Triassic
Pre-Mesozoic
Elevation (m)
Depth (m)

Fig. S.7. Topographical, geophysical, and longitudinal profiles of the entire 20.6-km length of the Veyron river in the westernmost of Switzerland. (a) One-km wide swath profile, showing three distinct positive reliefs along both sides of the river (labelled by V0, V1, and V2). The maximum and mean altitude curves show nearly the same pattern of change. (b) Longitudinal profile based on the channel's bottom elevation and gradient (SL index). (c) and (d) Unfiltered and filtered residual gravity and aeromagnetic anomaly profiles along the river path, respectively. (e) Geological cross-section along the river, extracted from a 3D geological model based on the interpretation of seismic reflection data (Gruber, 2017), showing that Cretaceous rock crops out in a small portion at both upper and lower parts of the profile. Red line represents a normal fault as suggested by Meier (2010).

Table A1

Name	Domain	CO	A	Hypsometric attributes			TTSI Analysis						
				HI	HS	HK	N	Az	M	Lmd	α95	α99	K
1	I	3rd	29.31	0.499	0.325	2.039	256	318.1	0.404	NW	1.8	2.2	25.7
							384	350.7	0.053	——	0.7	0.8	111.5
							278	38.5	0.42	NE	2.3	2.8	14.8
2	I	3rd	11.39	0.658	0.193	1.921	211	26	0.12	——	2.4	2.9	17.9
							208	74.5	0.654	~ E	2.3	2.8	19.6
3	I	3rd	32.94	0.433	0.526	2.195	185	322.3	0.019	——	2	2.4	28.7
4	I	4th	28.25	0.63	0.359	2.094	149	78.3	0.871	~ E	3.2	4	14.1
							172	208	0.039	——	1	1.2	116.8
5	II	4th	30.79	0.497	0.348	2.033	230	168.4	0.108	——	1.7	2.1	32.2
							84	136.1	0.884	SE	3	3.7	27.7
							86	215.6	0.762	SW	3.5	4.3	20.5
6	I	3rd	21.13	0.494	0.695	2.758	182	210.4	0.138	——	2	2.4	29.4
							219	37.4	0.52	NE	3.3	4.2	9.1
7	I	4th	28.87	0.433	0.721	2.623	547	141.5	0.1	——	1.1	1.3	32.1
							71	129	0.543	SE	2.3	2.9	54
8	I	3rd	29.65	0.448	0.585	2.285	210	107.9	0.13	——	2	2.5	25.1
9	I	3rd	20.28	0.526	0.579	2.417	509	234.4	0.249	SW	1.5	1.9	18.4
10	I	3rd	28.36	0.591	0.216	1.943	326	211	0.463	SW	1.8	2.2	20.7
							304	213.5	0.072	——	0.7	0.8	147.3
11	I	4th	27.38	0.646	0.247	1.98	196	49.6	0.266	NE	2.6	3.2	15.9
12	II	4th	32.01	0.55	0.332	1.988	61	256.4	0.166	——	2.2	2.8	66.8
							133	290.3	0.486	~W	3.8	4.7	11.6
13	II	3rd	26.31	0.576	0.359	2.043	132	348.7	0.044	——	1.5	1.9	65.2
							331	145	0.332	SE	1.6	2	23
14	II	3rd	66.66	0.458	0.458	2.044	242	232.6	0.492	SW	2.7	3.3	12.4
							319	288.1	0.028	——	0.8	1	91.3
							242	38.8	0.4	NE	2.5	3.1	14.2
15	II	4th	33.02	0.598	0.319	2.002	309	277.9	0.373	~ W	2.1	2.6	15.1
16	II	3rd	22.39	0.5	0.38	2.032	199	302.8	0.218	NW	2	2.5	26.4
17	II	4th	33.15	0.426	0.441	2.178	135	37.1	0.254	NE	2.9	3.2	22.6
18	II	4th	42.36	0.484	0.424	2.077	201	256.5	0.142	——	1.7	2.1	34.7
							211	271.6	0.608	~ W	2.7	3.4	13.7
19	II	3rd	32.58	0.64	0.326	2.036	451	108.7	0.419	~ E	2.4	3	8.6
							118	293.6	0.043	——	1.2	1.4	126.6
20	II	4th	52.19	0.472	0.41	2.109	510	318.2	0.282	NW	1.5	1.9	17.3
21	II	4th	54.27	0.542	0.261	1.871	578	319.9	0.127	——	0.9	1.1	46
22	II	4th	58.86	0.371	0.575	2.278	411	126.9	0.148	SE	0.8	1	80.9
23	II	4th	30.86	0.362	0.633	2.382	144	301.6	0.434	NW	3.8	4.7	10.6
24	II	4th	18.79	0.629	0.34	2.046	476	134.9	0.608	SE	1.6	1.9	18
25	II	3rd	18.04	0.64	0.232	1.925	178	141.3	0.606	SE	3	3.7	13.6
26	II	4th	18.13	0.534	0.304	1.948	327	100.7	0.021	——	1.6	2	25.3
							200	140.3	0.687	SE	2.9	3.6	13
27	I	4th	17.58	0.262	1.671	6.605	121	151	0.673	SE	3	3.7	19.2
28	I	4th	15.66	0.338	1.004	3.087	57	43.6	0.151	——	3.3	4.1	34.5
							105	206.4	0.543	SW	2.9	3.5	13.5
29	I	5th	14.05	0.483	0.46	2.146	102	324.4	0.473	NW	5.8	7.2	6.9
30	II	5th	37.17	0.633	0.305	2.015	73	307.7	0.016	——	1.4	1.7	148.1
							128	101.7	0.422	~ E	4.3	5.3	9.5
31	II	3rd	14.58	0.464	0.395	2.074	309	150.4	0.566	SE	2.7	3.4	9.6
32	II	4th	28.11	0.395	0.659	2.483	111	43	0.606	NE	4.4	5.5	10.3
							326	340.2	0.014	——	1.2	1.5	42.9
33	II	4th	81.22	0.421	0.306	1.952	345	89.5	0.242	~ E	2.4	2.9	11.3
34	II	4th	21.81	0.592	0.26	1.948	119	38.5	0.327	NE	4.4	5.4	9.7
35	II	4th	13.54	0.378	0.484	2.049	13	207.2	0.023	——	44	5.7	89.8
							101	155.8	0.728	SE	4.2	5.2	12.4
36	II	4th	28.82	0.654	0.298	2.065	426	167.5	0.197	~S	1.5	1.9	20.8
37	II	4th	34.79	0.458	0.369	2.012	174	324.6	0.114	——	1.5	1.8	54.6
38	II	5th	43.07	0.497	0.332	2.015	352	128.5	0.392	SE	2.4	3	10.3
39	II	4th	49.29	0.442	0.372	2.006	236	357.8	0.064	——	2.1	2.6	20.4
							167	125.7	0.591	SE	2.8	3.5	16
40	II	4th	37.28	0.439	0.394	2.057	355	302.5	0.363	NW	1.8	2.3	17.4
41	II	4th	27.93	0.389	0.447	2.14	275	202.7	0.211	SW	1.8	2.2	22.9
42	II	4th	47.23	0.419	0.473	2.159	88	68.8	0.314	~ E	2.9	3.6	27.8
							119	198.2	0.014	——	0.8	1	282.3
43	II	4th	22	0.449	0.384	2.054	405	339.3	0.09	——	1.8	2.3	15.6
44	II	3rd	18.54	0.621	0.341	2.076	226	145.5	0.442	SE	2.2	2.8	18.4
							82	156.9	0.106	——	1.4	1.8	120.6
45	II	3rd	25.47	0.372	0.421	2.039	386	305.4	0.2	NW	2.4	3	9.7
46	II	5th	9.93	0.546	0.393	2.113	144	110.3	0.052	——	1.1	1.3	123.8
47	II	3rd	12.18	0.624	0.28	1.998	162	115.2	0.08	——	1.3	1.6	72.8
							76	270.8	0.427	~W	3	3.7	30.2
48	I	3rd	7.4	0.648	0.226	1.962	68	316.1	0.798	NW	6	7.5	9.1
							29	144.7	0.177	——	6.2	7.8	19.7
49	I	3rd	3.34	0.476	0.386	2.002	27	294.4	0.06	——	3.3	4.2	72.1
							74	298.5	0.499	NW	3.9	4.9	18.8
50	I	5th	5.49	0.446	0.495	2.18	76	226.9	0.572	SW	4.1	5.1	16.6
							29	239.2	0.167	——	3.4	4.3	61.2
51	I	3rd	5.83	0.677	0.227	1.917	156	154.4	0.181	SE	3.1	3.9	13.9

52	I	3rd	9.97	0.528	0.338	1.936	125	146.9	0.326	SE	3.9	4.9	11.4
53	I	5th	12.03	0.292	0.661	2.342	88	84.9	0.074	——	1.7	2.2	75.4
54	I	3rd	11.91	0.458	0.49	2.152	83	153.1	0.347	SE	3.6	4.5	19.1
55	I	3rd	7.44	0.397	0.522	2.181	114	123.2	0.421	SE	4.1	5.1	11.4
56	I	4th	6.48	0.136	2.16	6.484	72	132.6	0.363	SE	4.2	5.2	17
57	I	3rd	7.98	0.655	0.235	1.974	56 63	144.2 24.3	0.707 0.042	SE ——	4.6 3.9	5.8 4.9	17.7 21.8
58	I	4th	12.62	0.26	1.052	3.342	——	——	——	——	——	——	——
59	I	3rd	11.64	0.406	0.613	2.5	84	227.4	0.246	SW	3.5	4.3	18
60	I	3rd	7.69	0.383	0.833	2.858	——	——	——	——	——	——	——
61	I	2nd	2.63	0.503	0.469	2.243	——	——	——	——	——	——	——
62	I	2nd	2.76	0.702	0.214	1.95	109	268.9	0.058	——	2.1	2.6	41.5
63	I	2nd	2.17	0.636	0.229	1.951	98	224.2	0.357	SW	4.4	5.4	11.6
64	I	5th	4.2	0.616	0.439	2.202	70 53	232 50.3	0.29 0.121	SW ——	3.5 2.8	4.3 3.5	24.7 50.5
65	I	3rd	4.33	0.596	0.222	1.855	136	46.6	0.036	——	1.9	2.4	40.3
66	II	3rd	12.46	0.621	0.289	2.021	25 104	35.2 257.9	0.0144 0.678	—— ~W	3.3 4.9	4.1 6.1	79.1 8.9
67	II	4th	14.88	0.477	0.447	2.124	36 114	14 305.2	0.03 0.654	—— NW	3.1 5.3	4 6.6	58.5 7.3
68	II	4th	14.93	0.231	0.55	2.113	109	329.7	0.403	NW	5.4	6.7	7.3
69	II	3rd	11.59	0.532	0.252	1.958	49 92	184.9 150.8	0.017 0.618	—— SE	2.6 4.9	3.3 6.1	60.6 10
70	II	3rd	9.8	0.699	0.248	1.985	139 59	290.6 167	0.368 0.04	~W ——	3.8 2	4.7 2.6	11.1 82.7
71	II	3rd	7.81	0.62	0.355	2.121	114	135.3	0.673	SE	4	5	11.7
72	II	2nd	6.34	0.531	0.389	2.106	38 44 61	288.3 147 301.5	0.06 0.813 0.474	—— SE NW	2.9 4.6 4.7	3.7 5.7 5.8	64.5 23.2 16.1
73	II	3rd	14.53	0.643	0.28	1.985	88 49	281.3 262.2	0.488 0.088	~W ——	4.9 2.3	6.2 2.9	10.3 79.1
74	II	3rd	5.25	0.446	0.589	2.384	57 79	167.6 188.7	0.106 0.784	—— ~S	3.3 4.8	4.1 6	34.3 12

Table A.1. Results of hypsometric and Transverse Topographic Symmetry Index (TTSI) analyses for seventy-four drainage catchments in the westernmost part of Switzerland. The following indications are reported: name of catchment; domain; CO: Catchment order (described by the highest order stream found within catchment according to Strahler method); A: Total catchment area in square kilometers; HI: Hypsometric Integral; HS: Hypsometric Skewness; HK: Hypsometric Kurtosis; N: Number of vectors; Az: directional mean vector according to Fisher distribution; M: Magnitude of mean vector according to Fisher distribution; Lmd: Lateral migration direction of drainage channel; α95 and α99 are respectively the angular radius, in degrees, of the 95% and 99% confidence cone around the mean; K: precision parameter. The level of confidence however describes precisely how well the mean is defined. Well-constrained clusters with well-defined mean vector are associated with small radius of confidence cones and high precision parameter (Borradaile, 2003). M values close or equal to zero indicate that stream flowing near catchment midline, while those values close or equal to one indicate that the stream flowing near the catchment boundary. NE: northeast; SE: southeast; NW: northwest; SW: southwest: W: west; E: east.